

Investigating Adsorbing Viscoelastic Fluids Using the Quartz Crystal Microbalance

Chris S. Hodges,* David Harbottle, and Simon Biggs



Cite This: *ACS Omega* 2020, 5, 22081–22090



Read Online

ACCESS |



Metrics & More

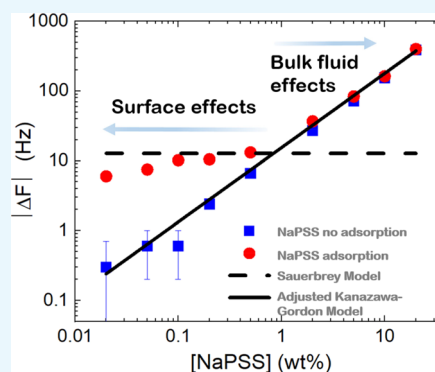


Article Recommendations



Supporting Information

ABSTRACT: There is little research on using the quartz crystal microbalance (QCM) with adsorbing viscoelastic fluids. These fluids are widely encountered but often difficult to study as many are opaque and highly viscous. Since the QCM does not involve any scattering or reflection of input radiation, it has the potential to study these complex fluids to determine the relative viscoelasticity of the bulk fluid and surface adsorption of active species onto different substrates. In the current study, both Newtonian (sucrose) and viscoelastic (sodium polystyrene sulfonate (NaPSS)) fluids were introduced into the QCM, and the sensor responses were compared. QCM responses of Newtonian sucrose solutions matched the Kanazawa and Gordon model (KG model), as expected. The QCM responses with viscoelastic NaPSS solutions were well below those described by the KG model. A viscoelastic model was used to determine the fluid viscosity and shear modulus at a very high frequency. It was found that the viscosity of NaPSS did not change much compared with low-frequency rheometer measurements, but a significant increase in the shear modulus of several orders of magnitude was found at the QCM frequencies. Modifying the KG model frequency shifts by multiplying by the QCM shear wave decay length ratio, $X = \delta_v/\delta_N$, we were able to match the measured QCM values in viscoelastic NaPSS solutions. The QCM dissipation values for NaPSS were matched in a similar way by multiplying the KG model by $X^{1/3}$. By changing the QCM sensor from silica (no NaPSS adsorption) to alumina (NaPSS adsorption), it was shown that the adsorption isotherm of NaPSS on alumina could be recovered and fitted with a Langmuir isotherm despite the frequency response being only a small fraction of the total measured QCM signal.



INTRODUCTION

The importance of complex surface active liquids (e.g., many commercially available polymer and/or surfactant-containing solutions) continues to grow as a result of their widespread use in products such as foods, agrochemical formulations, cosmetics, pharmaceutical dispersions, and personal care products.^{1,2} Control of the deposition behavior of the surface active species at the solid–liquid interface is frequently desired. Many of these complex formulations are highly viscous, containing components that readily adsorb to surfaces; however, knowledge of the interfacial behavior remains poor. The main difficulty in analyzing these types of fluids is that they often scatter radiation strongly, and therefore several common surface measurement techniques become unusable. The advantage of the quartz crystal microbalance (QCM) technique is that direct microscopic observation of the adsorption area is not required, and the scattering or reflection of input radiation is not needed. Hence, many liquids that cannot normally be investigated can, in principle, be analyzed.

Literature examples monitoring the adsorption of polyelectrolytes of the type used in the current study frequently consider the behavior at low concentrations using techniques such as ellipsometry, SAXS, SANS, and NMR. Although these polymer concentrations are below levels where the fluid

becomes rheologically interesting (usually $>C^*$, where C^* is the polymer chain overlap concentration), these data are useful in determining the adsorption mechanism, which is likely to remain consistent even if the bulk fluid begins to form long-range structures. Kawaguchi et al.³ showed through ellipsometry that adsorption of sodium polystyrene sulfonate (NaPSS) on platinum surfaces can create thin films between 10 and 80 nm thick depending on the molecular weight of NaPSS and the electrolyte concentration. Takahashi et al.⁴ used SANS to study the radius of gyration of NaPSS in aqueous and saline solutions at relatively low polymer concentrations. The authors observed a decrease in the radius of gyration at increasing polymer concentrations from about 13 to 5 nm. Cosgrove et al.⁵ used SANS to study NaPSS adsorption onto polystyrene (PS) particles. The authors determined that the adsorbed layer thickness varied according to the degree of sulfonation of the

Received: May 6, 2020

Accepted: August 13, 2020

Published: August 27, 2020



NaPSS, although the NaPSS molecules were always found to lie flat around the PS particles at all degrees of sulfonation. Using NMR, Smith et al.⁶ showed that NaPSS could be successfully deposited onto silica particles under suitable pH conditions, with the deposited layers found to be highly hydrated. Decher et al.⁷ are one of the few groups who have investigated polyelectrolyte layers deposited onto flat substrates by SAXS. The authors found that more than 40 layers of oppositely charged polyelectrolytes could be created with NaPSS and poly-4-vinylbenzyl(-*N,N*-diethyl-*N*-methyl) ammonium iodide, where the mean bilayer thickness was just over 2 nm. In all of these studies, the properties of the deposited layer were of primary interest, with the effect of the background solution being largely ignored.

Chiang et al.⁸ used optical tweezers to oscillate a 1.5 μm diameter polystyrene particle to determine G' and G'' in NaPSS solutions. Optical tweezers can access oscillation frequencies approximately 10 \times higher than rotational rheometers, and the particle used minimally disturbs the NaPSS fluid by only oscillating with an amplitude of about 36 nm. The authors identified the critical micelle concentration of 70 kDa NaPSS to be ~ 0.06 mM and the chain overlap concentration (C^*) to be ~ 1 mM, slightly higher than that reported by Boris and Colby⁹ (0.7 mM or ~ 5 wt %). Chiang et al.⁸ observed Rouse-like behavior (G' and $G'' \approx \omega^{0.5}$) up to ~ 1 mM NaPSS, above which the response changed to $G' \approx \omega$, which the authors claim is from chain entanglement and the formation of a transient network.

QCM studies using polyelectrolytes include Baba et al.¹⁰ who showed multilayer adsorption of PDADMAC and NaPSS onto gold sensors, where the bilayer thickness was calculated to be between 8 and 23 nm, with variation found between experiments. The adsorbed layer thickness was found to depend strongly on the polymer concentration (concentrations up to 0.2 wt % were tested). Naderi and Claesson¹¹ considered PVA–SDS complexes adsorbed onto polystyrene surfaces by a QCM at low polyelectrolyte concentrations (20 ppm) and found that the measured mass was very close to what would be expected for a thin viscoelastic adsorbed layer.¹² Tammelin et al.¹³ studied cationic starch films on silica by a QCM and successfully modelled the resultant frequency and dissipation shifts assuming the starch behaved as a viscoelastic thin film. Sadman et al.¹⁴ compared the well-known Voigt model with a power law model for the rheological properties of a thermally responsive copolymer in a Newtonian background fluid using QCM combined with an ellipsometry module. This setup allowed both light scattering data and QCM frequency and dissipation data to be collected simultaneously. The authors showed that both rheological models can follow the large changes in the modulus that occur during the swelling of the copolymer and that establishing a limit for the Sauerbrey model is important in understanding the adsorbed layer phase changes. Shull et al.¹⁵ used a QCM to study the rheological properties of polystyrene and poly(methyl methacrylate) thin films in water. The authors created software (RheoQCM) to automatically output the areal thickness, phase angle, and complex modulus of the adsorbed polymer film assuming a power law relationship for the rheological film behavior.

Each of the QCM studies described above use either a low concentration bulk solution or assume the background viscosity and density to be that of water. These studies demonstrate that viscoelastic and charged thin layers may be successfully adsorbed and modelled with meaningful output.

An area that has not received much scientific attention is the coupling of an adsorbed layer with a viscoelastic bulk fluid.

Mason et al.¹⁶ provided the first study of the shear properties of high viscosity fluids at ultrasonic frequencies. The authors showed that long-chain liquids such as castor oil exhibited a splitting between the resistance and the reactance of the measuring circuit demonstrating a viscoelastic liquid response, and this difference increased as the oscillation frequency increased. The characteristic impedance of the circuit and the liquid resonance response were directly related to the square root of the liquid density–viscosity product, a result reported by Kanazawa and Gordon¹⁷ nearly 40 years later. A range of poly(isobutylene) polymers at frequencies up to 50 MHz were also investigated, and since the phase angle at these high frequencies is small, accurate measurements of the pure circuit resistance could be measured: this is an early form of the Sauerbrey¹⁸ relation between the frequency and adsorbed mass. There is then a significant gap in the literature relating to high frequency studies of viscoelastic fluids until Borovikov and Peshkov investigated the temperature variation of the viscosity of solutions of ³He–⁴He mixtures¹⁹ in 1976. Nomura and Okuhara²⁰ immersed a QCM sensor in a wide range of non-adsorbing small molecule liquids with a wide range of solution viscosities and densities and showed that the observed frequency shifts were only dependent on the viscosity and density of the liquid. Calvo et al.²¹ described different versions of the Butterworth–van Dyke circuit analysis for thick (100 μm) viscoelastic oil films spread over the QCM sensor, showing that there is a phase shift induced in the shear modulus, which is dependent on the reactance and resistance of the QCM circuit and the density of the liquid. Thick (μm -sized) films of spin-cast poly(isobutylene) dried from toluene solutions have been studied by QCM to extract the deposited film compliance.²² Values of ~ 1 GPa⁻¹ were obtained by fitting viscoelastic models with different power law indices to the data. Johannsmann and co-workers²³ have investigated adsorbed polystyrene brushes in cyclohexane with the QCM. The authors found that the QCM response depends on the polymer brush length, in particular an increased frequency shift occurs when the brushes are one quarter of the Newtonian shear wave decay length. It is important to note that the QCM will, in general, probe the fluid to at least the shear wave penetration depth, $\delta_N = \sqrt{2\eta/\rho\omega}$ (Newtonian fluids), which is typically ~ 250 nm for a 5 MHz crystal in water at 20 °C. Fluid behavior beyond this depth may be detected but with significantly reduced QCM sensitivity.

Theoretical studies of viscoelastic films in contact with a liquid include a continuum mechanics model by Voinova et al.,²⁴ a mechanical model by Nwankwo and Durning,^{25–27} a fluid dynamics-based model by Krim and Widom,²⁸ and extensive work by Johannsmann et al.^{23,29–31} Very little experimental work, besides the early work of Mason et al.,¹⁶ has investigated the response of viscoelastic fluids with an adsorbed layer at the surface of the QCM sensor.

In the current study, the frequency and dissipation responses of silica and alumina sensors with unloaded resonant frequencies of 5 MHz were used with two fluids, sucrose and sodium polystyrene sulfonate (NaPSS). Since NaPSS is an anionic polyelectrolyte, it is expected to adsorb on alumina sensors but not on silica sensors, thus allowing the interaction between the QCM sensor and the bulk fluid to be modified. In

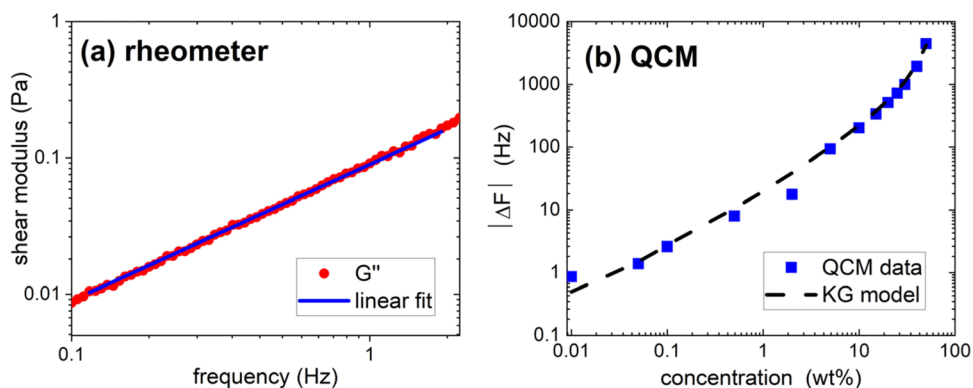


Figure 1. (a) Low-frequency oscillatory rheology of a 50 wt % sucrose solution showing the viscous modulus, G'' (red circles), versus oscillation frequency. Also shown is a linear fit to the data with a gradient of 1. (b) Magnitude of the QCM frequency responses at 15 MHz on a silica sensor as a function of the sucrose concentration and compared with the Kanazawa and Gordon (KG) model (eq 4).

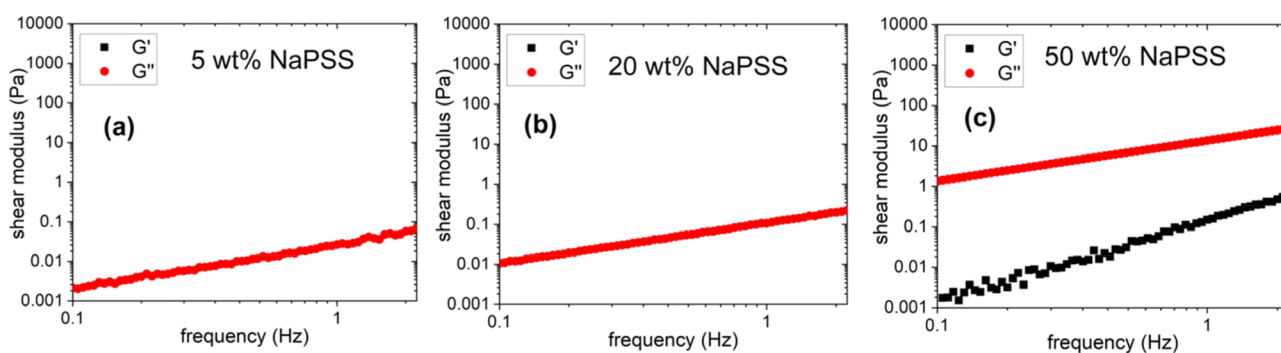


Figure 2. Low frequency oscillatory rheology of NaPSS solutions at (a) 5, (b) 20, and (c) 50 wt %. The viscous and elastic moduli are shown by the black square and red circle symbols, respectively.

addition, the nature of the background bulk fluid can be adjusted from Newtonian (sucrose) to viscoelastic (NaPSS).

RESULTS AND DISCUSSION

Frequency Response of a Newtonian Fluid—Sucrose.

Little reliable data is available for the rheological characterization of Newtonian fluids when subjected to an oscillatory excitation in the MHz frequency range. For the purpose of providing a reference, a 50 wt % sucrose solution was characterized at low frequencies by a rotational rheometer using a concentric cylinder geometry oscillating at frequencies between 0.1 and 2 Hz. An example of the low-frequency rheometer data (Figure 1a) is shown alongside the high-frequency QCM data for several sucrose solutions of increasing concentration (Figure 1b).

The low-frequency oscillatory rheology only has measurable G'' values (i.e., $G' \approx 0$) with a gradient of 1 on a log–log scale, as expected for a purely viscous Newtonian fluid. The 15 MHz QCM data demonstrates a good match to the KG model for Newtonian sucrose. These data show that sucrose remains Newtonian over a wide range of frequencies, from <1 Hz to at least 15 MHz. This is not surprising since the characteristic time for the permittivity of sucrose solutions is ~ 1 ns, corresponding to characteristic frequencies of around 1 GHz.³² The QCM dissipation data for sucrose (not shown) were also observed to fit the KG model. Johannsmann¹² shows that in Newtonian fluids, the complex fluid shear modulus, $\tilde{G}_1 = G' + iG''$ may be related to the fluid viscosity by $\sqrt{\rho_1 \tilde{G}_1} = \sqrt{i\omega\rho_1\eta_1}$ where $\omega = 2\pi f_0$, ρ_1 and η_1 are the density and viscosity of the

fluid, respectively, and f_0 is the unloaded resonant frequency of the QCM sensor. Given that in Newtonian fluids $G' = 0$, we have $G'' = \omega\eta_1$, which means that for a 50 wt % sucrose solution at 15 MHz, $G'' \approx 0.1$ GPa. This is similar to the shear modulus of solid PTFE, which demonstrates how stiff these fluids become when measured in the MHz range.

Frequency Response of a Viscoelastic Fluid—NaPSS.

The low-frequency oscillatory rheology of NaPSS solutions (Figure 2) shows a steady increase in G'' with an increasing NaPSS concentration. Only at 50 wt % NaPSS is the elastic contribution (G') measured by the rheometer. Chiang et al.⁸ presented rheological data on NaPSS measured by the optical tweezer technique, where even at very low NaPSS concentrations (<0.02 wt %) viscoelastic fluid properties (G' and G'') were measured. Unlike the rotational rheometer, the optical tweezers technique uses a small micron-sized bead with very low inertia and is therefore much more sensitive to changes in the fluid properties. This data is significant as it confirms that the NaPSS solutions are viscoelastic at very dilute concentrations.

Figure 3 shows that for all NaPSS concentrations, the measured frequency shifts at 15 MHz are much smaller than the values determined by the KG model. It should be noted that the frequency and dissipation shifts produced from 50 wt % NaPSS solutions were outside the measurement range of the QCM and thus have not been reported. The inset in Figure 3 shows that the absolute frequency difference between the KG model and the measured NaPSS data converges at low NaPSS concentrations. The instrument inertia of a QCM is much smaller than a rotational rheometer. This allows the QCM to

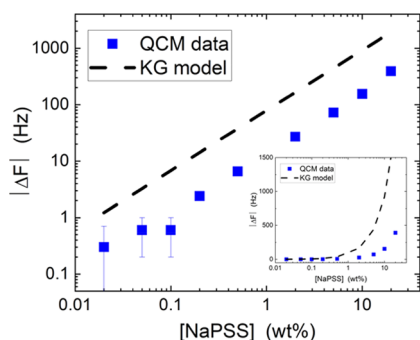


Figure 3. Magnitude of the QCM frequency responses (15 MHz, silica sensor) for NaPSS solutions of increasing concentration. The QCM frequency response is compared with the KG model (eq 4). The inset shows the same data on a semi-log plot.

be more sensitive to fluid properties even at very low fluid viscosities. Certainly at 5 and 20 wt %, the QCM demonstrates viscoelastic behavior, whereas the same fluids studied in a rheometer appear Newtonian (no G' in Figure 2a,b). In fact, Figure 3 suggests that at 15 MHz, the viscoelastic fluid behavior continues to at least 0.02 wt % NaPSS. This is interesting since the chain overlap concentration for 70 kDa NaPSS is ~ 10 wt %.³³ However, Chiang et al.⁸ showed that viscoelasticity can persist in NaPSS solutions down to very low concentrations (<0.02 wt %). The fact that the NaPSS frequency shifts are below those predicted by the KG model confirms that the QCM response is dominated by the bulk fluid effect and any possible ion adsorption (Na^+), which has been previously shown to modify the frequency response of a QCM,⁴¹ can be considered negligible.

Since NaPSS responds as a viscoelastic fluid at all measured frequencies, we may use the equations described by Johannsmann¹² for a viscoelastic fluid to obtain model values of viscosity at QCM frequencies. The complex viscosity $\tilde{\eta} = \eta' - i\eta''$

$$\eta'(\omega) = \frac{G''}{\omega} = -\frac{\pi\rho_q\mu_q}{\rho_l f_n} \frac{\Delta f_n \Delta\Gamma_n}{f_0^2} \quad (1)$$

$$\eta''(\omega) = \frac{G'}{\omega} = \frac{1}{2} \frac{\pi\rho_q\mu_q}{\rho_l f_n} \frac{\Delta\Gamma_n^2 - \Delta f_n^2}{f_0^2} \quad (2)$$

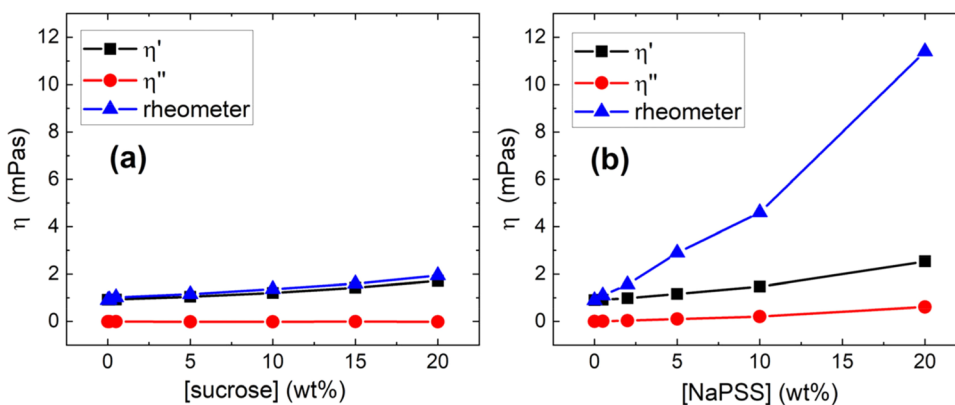


Figure 4. Dynamic viscosity, η' , and storage viscosity, η'' , calculated from QCM data at 15 MHz using eqs 1 and 2 for the cases of a silica sensor in (a) sucrose and (b) NaPSS solutions. The corresponding low-frequency viscosities measured using a rotational rheometer are also shown.

where ρ_q and μ_q are the quartz density and shear modulus, respectively, ρ_l is the density of the liquid, f_n is the frequency at overtone n , f_0 is the fundamental resonant frequency, Δf_n the measured frequency shift at overtone n , and $\Delta\Gamma_n (= \Delta D_{\eta} f_n / 2)$ is the measured change in the half bandwidth of the frequency spectrum at overtone n . Each of the viscosity components calculated from the QCM data is shown in Figure 4.

The sucrose data (Figure 4a) show excellent agreement between the calculated values of η' at 15 MHz and the low-frequency rheometer data. This shows that the sucrose dynamic viscosity is frequency independent, at least over the range of frequencies measured. The calculated η' values for the different concentrations of NaPSS at 15 MHz (Figure 4b) are of a similar magnitude but smaller than the low-frequency rheometer viscosities. Both η' and η'' increase slowly with an increasing NaPSS concentration. It is interesting to note that η' has very similar values for both sucrose and NaPSS over this concentration range, whereas η'' for NaPSS is small but nonzero, confirming the viscoelastic properties of this fluid. The differences between low (rheometer) and high (QCM) frequency η'' values for NaPSS solutions are probably related to molecular structuring effects³⁵ and the vicinity of the bulk fluid to the sensor surface, neither of which are included in the model (eqs 1 and 2). This shows the potential advantage of using QCM to study viscoelastic fluids, particularly near to a surface.

We can use the calculated high frequency values of η' and η'' for NaPSS solutions (Figure 4b) to determine values of G'' and G' using eqs 1 and 2, respectively (Figure 5).

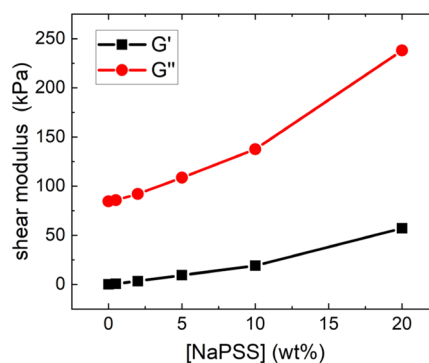


Figure 5. Calculated shear moduli, G' and G'' , determined using eqs 1 and 2. QCM data used was NaPSS solutions at 15 MHz on silica.

The calculated values of G' and G'' (Figure 5) show a monotonic increase with the NaPSS concentration. The absolute values of G'' are much larger than those obtained at low frequencies measured using the rheometer (Figure 2). In fact, G'' increases to ~ 0.25 MPa at 20 wt % NaPSS, which is similar to a typical soft solid. The ability of the QCM to measure G' values down to 0.02 wt % NaPSS is demonstrated and confirms the higher measurement sensitivity of the QCM compared to a rotational rheometer. Both moduli vary with frequency, with $G' \approx \omega^{0.3}$ and $G'' \approx \omega^{0.9}$ (see the Supporting Information, Figure S3).

Quantification of Fluid Viscoelasticity in a QCM. The shear wave emanating from the QCM sensor surface into a Newtonian fluid has a decay length, $\delta_N = \sqrt{2\eta/\omega\rho}$, for fluid viscosity η , fluid density ρ , and angular frequency $\omega = 2\pi f_m$, corresponding to $\delta_N = 145$ nm at 15 MHz for a fluid with the density and viscosity of water. For viscoelastic fluids, Johannsmann et al.¹² state that the shear wave penetration depth is given by $\delta_V = \frac{1}{k''} = -\frac{1}{\omega\sqrt{\rho}} \frac{|\tilde{G}_1|}{\text{Im}(\sqrt{\tilde{G}_1})}$, where $\tilde{G}_1 = G' + iG''$. For a 20 wt % NaPSS solution at 15 MHz, $\delta_V \approx 9$ nm. We define $X = \delta_V/\delta_N$ and, using a single value for X evaluated at 20 wt % NaPSS, plot $X\Delta f_{\text{KG}}$ (referred to as the adjusted KG model) versus the NaPSS concentration alongside the same NaPSS QCM data shown in Figure 3.

Figure 6 shows that by multiplying the KG model frequency shifts at 15 MHz by X , the adjusted KG model overlaps the

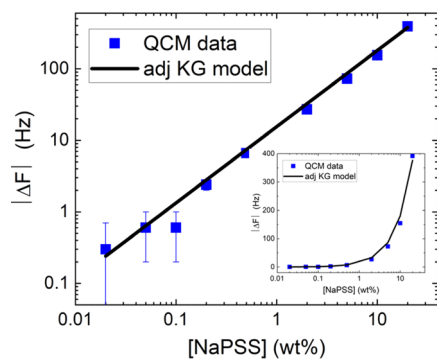


Figure 6. Magnitude of the QCM frequency responses (15 MHz, silica sensor) for NaPSS solutions of increasing concentration. Also plotted are the adjusted KG model frequency shifts. The inset shows the same data on a semi-log plot.

measured frequency shifts. Thus, for any particular fluid, a value of δ_N and δ_V may be found, and a simple adjustment to the Newtonian KG model can be made to fit viscoelastic fluids at QCM frequencies. In the current study, the QCM frequency response to NaPSS concentration varied as $[\text{NaPSS}]^{0.5}$ and so, a single value of $X = 0.065$ was sufficient to fit the data. We note that both δ_N and δ_V are frequency dependent, so the different QCM harmonics would generate new values for X . However, the change in X with QCM frequency was found to be negligible over the frequency range (see the Supporting Information, Figure S2). We also provide a similar treatment to the KG model dissipation values (adj KG model), as shown in Figure 7.

Figure 7 shows that the KG model dissipation is consistently above the measured QCM dissipation, although the data do seem to follow a $[\text{NaPSS}]^{0.5}$ dependence, as was found for the frequency data (Figure 6). If we consider the case of a finite

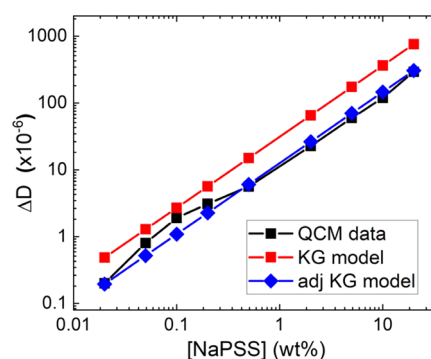


Figure 7. QCM dissipation response (15 MHz, silica sensor) for NaPSS solutions of increasing concentration. Also presented are the KG model dissipation values (red) and the adjusted KG model dissipation values (blue).

viscoelastic layer in the QCM,²⁴ then $\Delta D_V = X^{1/3}\Delta D$. Since the KG model is parallel to the measured dissipation values, a single value of X can be used to adjust the KG model dissipation values. The adjusted KG model fits the measured data well.

As an important aside, we note that δ_V can become very short, just a few nm. Nanoscale forces between silica surfaces have been previously measured in NaPSS solutions,³⁶ and it was found that a region depleted of NaPSS exists that is 10 nm thick at 1 wt % NaPSS and 30 nm thick at 0.1 wt % NaPSS. This implies that the locality of the bulk NaPSS molecular structure to the QCM sensor surface becomes comparable to the viscoelastic shear wave penetration depth in the higher concentration NaPSS solutions. One way to study the effect of locality of the bulk solution to the QCM sensor is to alter the type of sensor surface.

Effect of an Adsorbed Layer in a Viscoelastic Fluid.

Unlike sucrose, NaPSS selectively adsorbs depending on the surface type. Two types of QCM sensors, silica and alumina, were selected to compare the frequency and dissipation responses in a viscoelastic fluid at high (MHz) frequencies with adsorption (alumina) and without adsorption (silica) of NaPSS.

Figure 8 shows that for low NaPSS concentrations (< 1 wt %), differences in both Δf and ΔD are measured when the QCM sensor is changed from silica (no NaPSS adsorption) to alumina (NaPSS adsorption). For the alumina sensor, the frequency data below 1 wt % NaPSS represents the adsorption isotherm of NaPSS at 20 °C, rising up to a plateau frequency equivalent to a 0.9 nm-thick Sauerbrey film (Sauerbrey line in Figure 8). The calculated film thickness agrees with the existing literature for NaPSS where values of ~ 1 nm are typical.

When the solution concentration of NaPSS is above 1 wt %, both surfaces follow the same trend and show a $[\text{NaPSS}]^{0.5}$ dependence, following the adjusted KG model line. Thus, we have shown that irrespective of the QCM sensor surface type (silica or alumina), the same frequency response to the bulk viscoelastic fluid occurs. This agrees with our earlier hypothesis that most of the QCM response to viscoelastic fluids is from the bulk solution rather than the sensor surface. If we take the difference between the frequency data on alumina and silica, we then recover the surface adsorption isotherm (Figure 9).

The Langmuir isotherm fits the frequency data reasonably well, demonstrating that NaPSS readily adsorbs on alumina,

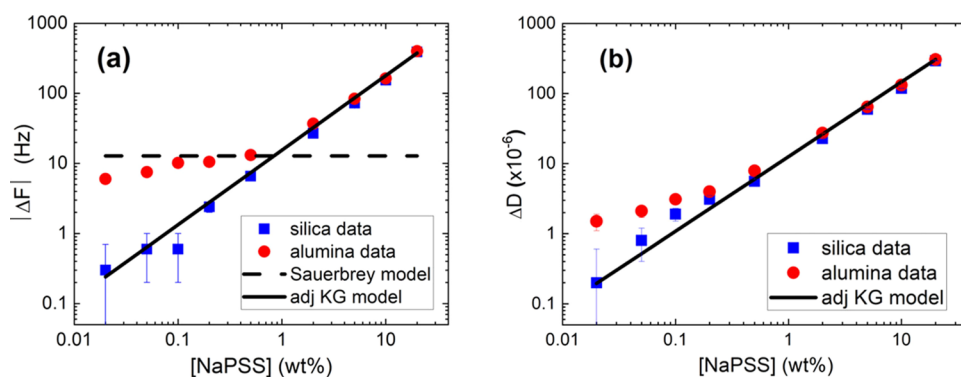


Figure 8. QCM data at 15 MHz showing the (a) magnitude of frequency shifts and (b) dissipation shifts measured in NaPSS solutions of various concentrations on either a silica (blue) or alumina (red) QCM. Also shown are the adjusted KG model frequency and dissipation shifts (see Figures 6 and 7). For details of the Sauerbrey line, see the text.

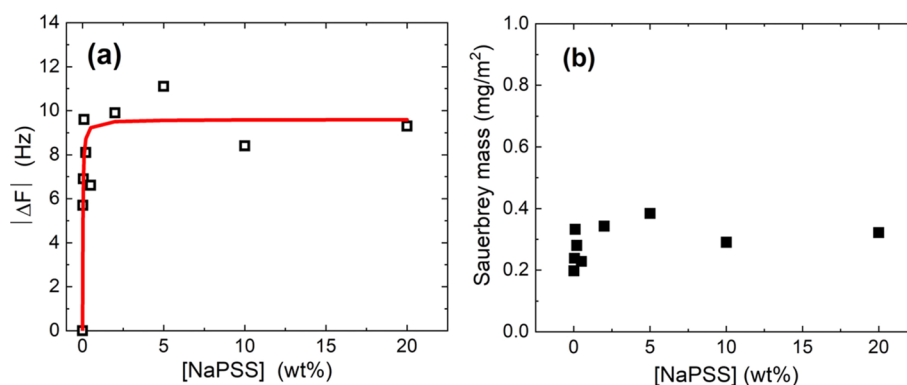


Figure 9. (a) Difference between the measured QCM frequency shifts at 15 MHz for NaPSS on alumina and silica surfaces as a function of the NaPSS concentration. The red line is a Langmuir isotherm fit to the experimental data. (b) Corresponding calculated Sauerbrey mass for NaPSS adsorption on the alumina QCM sensor.

reaching a plateau at ~ 0.2 wt % NaPSS. The corresponding Sauerbrey mass calculated for the adsorbed layer is very small at only 0.3 mg/m^2 , very similar to ellipsometry values obtained by Kawaguchi et al.,³ strongly suggesting that a very low density, open-structured layer forms on alumina.

The dissipation data in Figure 8b also show a response to the surface type below 1 wt % NaPSS, with alumina producing larger changes in ΔD than silica due to the adsorption of NaPSS on this surface. Above 1 wt % NaPSS, the dissipation data follow a $[\text{NaPSS}]^{0.5}$ dependence, in the same way as the frequency data. As a measure of the degree of viscoelasticity in the NaPSS solutions, we plot the proximity of the experimental NaPSS data to the KG model (i.e., measured value/KG model value $\times 100$) in Figure 10.

In Figure 10, 100% on the ordinate represents a Newtonian fluid. The frequency shifts for both alumina and silica surfaces lie very close to each other above 5 wt % NaPSS, demonstrating a constant degree of fluid viscoelasticity at approximately 18% of the KG model. Below 5 wt % NaPSS, the frequency data diverge for each surface due to the adsorption on alumina but not on silica. Figure 10 suggests that it is reasonable to use a simple addition model of the surface adsorption plus the (viscoelastic adjusted) bulk fluid response, similar to the idea put forward by Urbakh.³⁴

By comparison, the dissipation responses (Figure 10) are significantly different depending on the sensor type, even at high NaPSS concentrations. It is likely that this difference between silica and alumina results from (i) the coupling

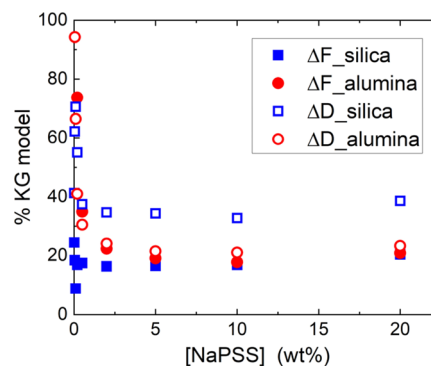


Figure 10. Ratio of the measured frequency and dissipation shifts to the KG model on silica (blue squares) and alumina (red circles) QCM sensors as a function of the NaPSS concentration.

strength of the NaPSS molecules to the QCM sensor and (ii) the proximity of the bulk fluid molecular structure to the QCM sensor, i.e., the depletion length. Note that the semi-infinite viscoelastic model¹² used in the current study does not account for these mechanisms but instead predicts identical dissipation responses irrespective of the QCM sensor type. However, since the dissipation (or bandwidth) is sensitive to the viscoelasticity of the adsorbed layer, localized changes in the molecular bonding or structure will be sensed much more than the frequency, particularly since the viscoelastic shear wave decay length, δ_v , is so small ($\sim 10 \text{ nm}$) at 15 MHz.

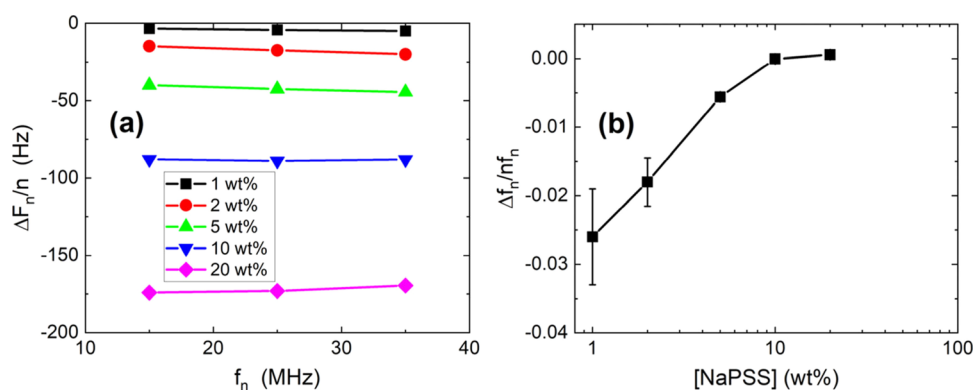


Figure 11. (a) QCM frequency data for different NaPSS concentrations adsorbed onto an alumina sensor versus the resonance frequency at three overtones of the QCM sensor. (b) Slope ($\Delta f_n/nf_n$) from panel (a) as a function of the NaPSS concentration (wt %).

Johannsmann¹² describes a useful way of examining an adsorbed viscoelastic layer from a fluid, which may relate to our case of NaPSS on alumina. If the normalized frequency shifts, $\Delta f_n/n$, are plotted versus the overtone, n (Figure 11a), then the slope of the resultant line may be related to J'' , the imaginary (elastic) part of the compliance of the adsorbed film. Johannsmann intimates that if a constant value (zero gradient) is found, then it results in a frequency-independent elastic compliance of the adsorbed film (i.e., the film behaves as a Sauerbrey inertial mass). Soft adsorbed layers usually produce positive gradients.

Figure 11a shows the measured frequency response of each NaPSS concentration for three different overtones. The slope ($\Delta f_n/nf_n$) of each line is shown in Figure 11b. With an increasing NaPSS concentration, the negative slope decreases, passing through a zero gradient at 10 wt % NaPSS. It should be noted that all NaPSS concentrations in Figure 11 are well above those considered by Johannsmann;¹² therefore, our case is of an adsorbed thin film in a highly viscoelastic bulk fluid (rather than a Newtonian bulk fluid). We have already shown that in these fluids, the QCM is mainly sensitive to the bulk, and the effect of the sensor type is relatively small. Therefore, instead of Figure 11b examining the response of the adsorbed NaPSS layer, it may be that the change in the gradient in Figure 11 is related to the proximity of the bulk molecular structure above the adsorbed layer, in which case Figure 11b provides a possible mechanism for estimating the depletion length of the polymer. As calculated earlier, at 15 MHz, $\delta_V \approx 10$ nm, and at 25 and 35 MHz, the viscoelastic shear wave decay lengths are even shorter, 5.6 and 4 nm, respectively. As the NaPSS concentration increases, the depletion length at the QCM sensor–fluid interface decreases, so when each overtone has an equivalent frequency shift, the bulk fluid structure is being sensed equally by the QCM. For the case of NaPSS, the QCM detects equal overtone responses at 10 wt % (Figure 11b), so the NaPSS depletion length at 10 wt % must be ≤ 4 nm. If this approach is valid, then it represents a completely novel method to estimate depletion lengths of complex viscoelastic fluids at high solution concentrations.

CONCLUSIONS

Experiments have been conducted to compare low-frequency rheometer measurements with high-frequency QCM measurements of a Newtonian fluid (sucrose) and a viscoelastic fluid (NaPSS). For sucrose, the low-frequency rheology showed

only a G'' response (i.e., $G' = 0$) as expected for a Newtonian fluid. QCM measurements at 15 MHz obeyed the Newtonian KG model, demonstrating that sucrose remains a Newtonian fluid up to at least 15 MHz. By comparison, the low-frequency rheology for NaPSS showed a gradual increase in G'' with increasing NaPSS concentration, and only at 50 wt % NaPSS was the solution viscosity high enough to measure a G' contribution. For NaPSS, the high-frequency QCM data were much smaller than predicted by the KG model (both frequency and dissipation).

A viscoelastic model was applied to the QCM data to calculate the solution viscosity and from these values, the solution shear modulus was calculated, allowing comparison of the high-frequency QCM data and the low-frequency rheometer data. The calculated viscosities from the QCM data for both sucrose and NaPSS solutions were close to the rheometer values despite the large difference in measurement frequency (Hz for the rheometer, MHz for the QCM). However, there was a large difference in the shear modulus for 20 wt % NaPSS (<0.1 Pa from the rheometer, ~ 250 kPa from the QCM). By defining the ratio of shear wave decay lengths in viscoelastic and Newtonian fluids to be $X = \delta_V/\delta_N$ and multiplying X by the KG model frequency shift, Δf_{KG} , good agreement was found with the measured QCM frequency shifts in NaPSS solutions. When $X^{1/3}$ was multiplied by the KG model dissipation shifts, good agreement was found with the measured QCM dissipation shifts in NaPSS solutions.

By changing the QCM sensor type from silica (no NaPSS adsorption) to alumina (NaPSS adsorbs), it was found that above 1 wt % NaPSS, most of the QCM response comes from the bulk solution rather than the surface. Despite the interfacial contribution being only a small fraction of the total QCM response, the adsorption isotherm of NaPSS on alumina could be recovered by subtracting the silica frequency data from the alumina frequency data. With adsorption of NaPSS on alumina, an overtone-dependent frequency shift diminished with increasing NaPSS concentration. At 10 wt % NaPSS, the measured frequency shift at each overtone was the same, demonstrating a uniform sensing of the bulk fluid. We hypothesize that this frequency response is a function of the locality of the bulk fluid to the sensor and, based on the highest measured frequency (35 MHz), estimate that the depletion length is ≤ 4 nm. This analysis may represent a novel way to study depletion lengths in high-concentration viscoelastic fluids, which is currently very difficult to achieve.

MATERIALS AND METHODS

Sucrose was used as a typical Newtonian fluid, and solutions were made in concentrations from 0.01 to 50 wt% with ultrapure Milli-Q water (pH: ~ 5.5 , resistivity: $>10^{18}$ Ωcm). Sodium polystyrene sulfonate (NaPSS) solutions were prepared in concentrations from 0.02 to 20 wt%. The 70 kDa NaPSS and sucrose powders were purchased from Sigma-Aldrich and used as received without further purification. The bulk properties (density and viscosity) of the sucrose solutions used were taken from the CRC Handbook of Chemistry and Physics.³⁷ The density of the NaPSS solutions was measured using a Micromeritics Accupyc 1330 pycnometer.

The low-frequency shear modulus was measured using a TA Instruments Discovery HR-2 rheometer, with the bearing mode set to soft for maximum measurement sensitivity. The fluid viscous (G') and elastic (G'') shear moduli were measured using a logarithmic frequency sweep between 0.1 and 100 Hz with 100 points per decade and an averaging time of 30 s per point. All experiments were conducted at $T = 25$ °C. Note that for the lowest concentrations of NaPSS used (0.02 wt %), the measured viscosity and density values were indistinguishable from water within the uncertainty of the measurement (approximately 1 and 0.03% for the viscosity and density, respectively).

The QCM includes an AT-cut quartz sensor that is set to vibrate laterally in shear thickness mode at its fundamental resonant frequency of 5 MHz. In the current study, data is presented for the third overtone at 15 MHz since it provides the best signal-to-noise ratio. Frequency and dissipation shifts were made from a water background. By measuring the frequency response in different gaseous environments with respect to the adsorbed mass of the particular gas molecule, Sauerbrey found that the frequency response, Δf , varies linearly with added mass, Δm , at overtone, n , as¹⁸

$$\frac{\Delta f}{n} = \frac{-\Delta m}{C_s} \quad (3)$$

where C_s is the sensitivity constant for the QCM sensor (18 $\text{ng cm}^{-2} \text{Hz}^{-1}$), which is related to the physical properties of the quartz and the fundamental frequency of oscillation of the sensor.

Kanazawa and Gordon¹⁷ showed through a simple one-dimensional shear wave model for a semi-infinitely thick Newtonian liquid layer, and the measured frequency shift, Δf , from the background solvent is

$$\frac{\Delta f}{\sqrt{n}} = -f_0^{3/2} \sqrt{\frac{1}{\pi\mu_q\rho_q}} (\sqrt{\rho_l\eta_l} - 1) \quad (4)$$

where f_0 is the fundamental resonance frequency of the sensor, μ_q and ρ_q are the shear modulus and density of the QCM sensor, and ρ_l and η_l are the density and viscosity of the fluid, respectively. This will be referred to as the KG model. Eq 4 shows that for any particular non-adsorbing liquid interacting with the QCM sensor, the ratio $\frac{\Delta f}{\sqrt{n}}$ depends entirely on the density–viscosity product of the bulk fluid. Moreover, if the fluid density–viscosity product changes linearly with increasing fluid concentration, then a straight line with a gradient of 0.5 should result. Note that this model assumes the fluid is in perfect contact with the QCM sensor and is completely isotropic and Newtonian. In eq 4, the shear modulus μ_q (2.9×10^{10} $\text{kg m}^{-1} \text{s}^{-2}$) and density ρ_q (2648 kg m^{-3}) of the quartz

sensor is combined with the fundamental resonant frequency of the sensor f_0 to give a modified sensitivity C_{KG} for the KG model, where $\frac{1}{C_{\text{KG}}} = f_0^{3/2} \sqrt{\frac{1}{\pi\mu_q\rho_q}}$ ($= 709$ $\text{m}^2 \text{kg}^{-1} \text{s}^{-1/2}$).

The E4 QCM (Q-Sense, Sweden) has four cells that may be used in parallel. In the current study, only one cell was used for simplicity and reproducibility. The liquid to be measured was flowed into the QCM cell at a flow rate of 0.12 mL/min, and the cell was maintained at 25 °C throughout the experiment. In a typical experiment, the empty cell was first filled with Milli-Q water until stable frequency and dissipation values were attained. This initial air-to-water experiment was then stopped and recorded each time. The adsorption experiment was then started with the cell filled with flowing Milli-Q water. After a few minutes, the sample liquid was introduced into the cell, and the frequency and dissipation values were again allowed to equilibrate. Milli-Q water was then re-introduced into the cell to rinse out the sample until the frequency and dissipation values had returned to the values at the start of the experiment. This procedure was carried out sequentially with different samples over the entire concentration range of the test fluids. The dissipation signal, ΔD , is related to the bandwidth of the sensor resonance, $\Delta\Gamma$, by $\Delta D = 2\Delta\Gamma/f_0$.

The fundamental resonance frequency of the 14 mm quartz sensor was near 5 MHz (~ 4.95 MHz). Alumina- and silica-coated sensors were supplied by Q-Sense. At the unadjusted pH of Milli-Q water (pH = 5.5), the silica sensor was negatively charged, and the alumina sensor was positively charged.^{38,39} All sensors were cleaned following the procedure previously described.⁴⁰

ASSOCIATED CONTENT

Supporting Information

The Supporting Information is available free of charge at <https://pubs.acs.org/doi/10.1021/acsomega.0c02100>.

(Figure S1) QCM response of NaPSS on the silica sensor for increasing NaPSS concentrations showing the (a) raw frequency and (b) dissipation values for the third, fifth, and seventh overtones; (Figure S2) variation of X versus QCM measurement frequency also showing the slope of the fitted line; and (Figure S3) NaPSS solution modulus versus measurement frequency for a 20 wt % NaPSS solution showing the slopes of each line the figure (PDF)

AUTHOR INFORMATION

Corresponding Author

Chris S. Hodges – School of Chemical and Process Engineering, University of Leeds, Leeds LS2 9JT, United Kingdom; orcid.org/0000-0002-2252-8645; Email: pmcsh@leeds.ac.uk

Authors

David Harbottle – School of Chemical and Process Engineering, University of Leeds, Leeds LS2 9JT, United Kingdom; orcid.org/0000-0002-0169-517X

Simon Biggs – School of Chemical and Process Engineering, University of Leeds, Leeds LS2 9JT, United Kingdom

Complete contact information is available at: <https://pubs.acs.org/doi/10.1021/acsomega.0c02100>

Notes

The authors declare no competing financial interest.

ACKNOWLEDGMENTS

The authors thank Scientific and Medical Products Ltd. (SciMed), for helping with the QCM setup.

REFERENCES

- (1) Dickinson, E. *Food Polymers, Gels and Colloids*; Dickenson, E. (Ed.), Special Publication No. 82, Royal Society of Chemistry: Cambridge, 1991.
- (2) *Rheological Properties of Cosmetics and Toiletries*; Laba, D. (Ed.) Marcel Dekker: New York, 1993.
- (3) Kawaguchi, M.; Hayashi, K.; Takahashi, A. Effects of molecular weight and salt concentration on the thickness of sodium poly(styrene sulphonate) adsorbed on a metal surface: 3. Comparison with scaling concepts. *Macromolecules* **1984**, *17*, 2066–2070.
- (4) Takahashi, Y.; Matsumoto, N.; Iio, S.; Kondo, H.; Noda, I.; Imai, M.; Matsushita, Y. Concentration dependence of radius of gyration of sodium poly(styrene sulphonate) of a wide range of concentration studied by small angle neutron scattering[†]. *Langmuir* **1999**, *15*, 4120–4122.
- (5) Cosgrove, T.; Obey, T. M.; Vincent, B. The configuration of poly(styrene sulphonate) at polystyrene/solution interfaces. *J. Colloid Interface Sci.* **1986**, *111*, 409–418.
- (6) Smith, R. N.; McCormick, M.; Barrett, C. J.; Reven, L.; Spiess, H. W. NMR studies of PAH/PSS polyelectrolyte multilayers adsorbed onto silica. *Macromolecules* **2004**, *37*, 4830–4838.
- (7) Decher, G.; Hong, J. D.; Schmitt, J. Build-up of ultra-thin multilayer films by a self-assembly process: III Consecutively alternating adsorption of anionic and cationic polyelectrolytes on charged surfaces. *Thin Solid Films* **1992**, *210-211*, 831–835.
- (8) Chiang, C.-C.; Wei, M.-T.; Chen, Y.-Q.; Yen, P.-W.; Huang, Y.-C.; Chen, J.-Y.; Lavastre, O.; Guillaume, H.; Guillaume, D.; Chiou, A. Optical tweezers based active microrheology of polystyrene sulfonate (NaPSS). *Opt. Express* **2011**, *19*, 8847–8854.
- (9) Boris, D. C.; Colby, R. H. Rheology of sulfonated polystyrene solutions. *Macromolecules* **1998**, *31*, 5746–5755.
- (10) Baba, A.; Kaneko, F.; Advincula, R. C. Polyelectrolyte adsorption processes characterized in situ using the quartz crystal microbalance technique: alternate adsorption properties in ultrathin polymer films. *Colloids Surf., A* **2000**, *173*, 39–49.
- (11) Naderi, A.; Claesson, P. M. Adsorbed properties of polyelectrolyte-surfactant complexes on hydrophobic surfaces studied by QCM-D. *Langmuir* **2006**, *22*, 7639–7645.
- (12) Johannsmann, D. *The Quartz Crystal Microbalance in Soft Matter Research: fundamentals and modeling*; p208, p232, Springer: 2015.
- (13) Tammelin, T.; Merta, J.; Johansson, L.-S.; Stenius, P. Viscoelastic properties of cationic starch adsorbed on quartz studied by QCM-D. *Langmuir* **2004**, *20*, 10900–10909.
- (14) Sadman, K.; Wiener, C. G.; Weiss, R. A.; White, C. C.; Shull, K. R.; Vogt, B. D. Quantitative rheometry of thin soft materials using the quartz crystal microbalance with dissipation. *Anal. Chem.* **2018**, *90*, 4079–4088.
- (15) Shull, K. R.; Taghon, M.; Wang, Q. Investigations of the high frequency dynamic properties of polymeric systems with quartz crystal resonators. *Biointerphases* **2020**, *15*, No. 021012.
- (16) Mason, W. P.; Baker, W. O.; McSkimin, H. J.; Heiss, J. H. Measurement of elasticity and viscosity of liquids at ultrasonic frequencies. *Phys. Rev.* **1949**, *75*, 936–946.
- (17) Kanazawa, K. K.; Gordon, J. G., II The oscillation frequency of a quartz crystal in contact with a liquid. *Anal. Chim. Acta* **1985**, *175*, 99–105.
- (18) Sauerbrey, G. Verwendung von Schwingquarzen zur Wägung Dünner Schichten und zur Mikrowägung. *Z. Phys.* **1959**, *155*, 206–222.
- (19) Borovikov, A. P.; Peshkov, V. P. Interaction between an oscillating solid wall and a ³He-⁴He solution. *JETP* **1976**, *43*, 156–161.
- (20) Nomura, T.; Okuhara, M. Frequency shifts of piezoelectric quartz crystals immersed in organic liquids. *Anal. Chim. Acta* **1982**, *142*, 281–284.
- (21) Calvo, E. J.; Etchenique, R.; Bartlett, P. N.; Singhal, K.; Santamaria, C. Quartz crystal impedance studies at 10 MHz of viscoelastic liquids and films. *Faraday Discuss.* **1997**, *107*, 141–157.
- (22) Johannsmann, D. Viscoelastic analysis of organic thin films on quartz resonators. *Macromol. Chem. Phys.* **1999**, *200*, 501–516.
- (23) Wolff, O.; Seydel, E.; Johannsmann, D. Viscoelastic properties of thin films studied with quartz crystal resonators. *Faraday Discuss.* **1997**, *107*, 91–104.
- (24) Voinova, M. V.; Rodahl, M.; Jonson, M.; Kasemo, B. Viscoelastic acoustic response of layered polymer films at fluid-solid interfaces: continuum mechanics approach. *Phys. Scr.* **1999**, *59*, 391–396.
- (25) Nwankwo, E.; Durning, C. J. Mechanical response of thickness-shear mode quartz crystal resonators to linear viscoelastic fluids. *Sens. Actuators A* **1998**, *64*, 119–124.
- (26) Nwankwo, E.; Durning, C. J. Fluid property investigation by impedance characterization of quartz crystal resonators. Part II: parasitic effects, viscoelastic fluids. *Sens Actuators A* **1999**, *72*, 195–202.
- (27) Nwankwo, E.; Durning, C. J. Impedance analysis of thickness-shear mode quartz crystal resonators in contact with linear viscoelastic media. *Rev. Sci. Instrum.* **1998**, *69*, 2375–2384.
- (28) Krim, J.; Widom, A. Damping of a crystal oscillator by an adsorbed monolayer and its relation to interfacial viscosity. *Phys. Rev. B* **1988**, *38*, 12184–12189.
- (29) Pax, M.; Rieger, J.; Eibl, R. H.; Thielemann, C.; Johannsmann, D. Measurements of fast fluctuations of viscoelastic properties with the quartz crystal microbalance. *The Analyst* **2005**, *130*, 1474–1477.
- (30) Johannsmann, D.; Mathauer, K.; Wegner, G.; Knoll, W. Viscoelastic properties of thin films probed with a quartz crystal resonator. *Phys. Rev. B* **1992**, *46*, 7808–7815.
- (31) König, A. M.; Düwel, M.; du, B.; Kunze, M.; Johannsmann, D. Measurements of interfacial viscoelasticity with a quartz crystal microbalance: influence of acoustic scattering from a small crystal-sample contact. *Langmuir* **2006**, *22*, 229–233.
- (32) Guo, W.; Liu, Y.; Zhu, X.; Wang, S. Dielectric properties of honey adulterated with sucrose syrup. *J. Food Eng.* **2011**, *107*, 1–7.
- (33) Dobrynin, A. V.; Colby, R. H.; Rubinstein, M. Scaling theory of polyelectrolyte solutions. *Macromolecules* **1995**, *28*, 1859–1871.
- (34) Urbakh, M. *Probing the solid/liquid interface with the quartz crystal microbalance piezoelectric sensors*; Steinem, C.; Janshoff, A. (Eds.), (2007), p123.
- (35) Spiteri, M. N.; Williams, C. E.; Boué, F. *Pearl necklace-like chain conformation of hydrophobic polyelectrolyte: a SANS study of partially sulphonated polystyrene in water*; <https://arxiv.org/pdf/0904.2641> 2009.
- (36) Biggs, S.; Burns, J. L.; Yan, Y.-l.; Jameson, G. J.; Jenkins, P. Molecular weight dependence of the depletion interaction between silica surfaces in solutions of sodium poly(styrene sulphonate). *Langmuir* **2000**, *16*, 9242–9248.
- (37) Hayes, A. W. *CRC Handbook of Chemistry and Physics*; 95th Edition, 2014-2015, 5–145.
- (38) Tewari, P. H.; McClean, A. W. Temperature dependence of point of zero charge of alumina and magnetite. *J. Colloid Interface Sci.* **1972**, *40*, 267–272.
- (39) Schwarz, J. A.; Driscoll, C. T.; Bhanot, A. K. The zero point of charge of silica-alumina oxide suspensions. *J. Colloid Interface Sci.* **1984**, *97*, 55–61.
- (40) Biggs, S.; Labarre, M.; Hodges, C.; Walker, L. M.; Webber, G. B. Polymerised rod-like micelle adsorption at the solid-liquid interface. *Langmuir* **2007**, *23*, 8094–8102.

(41) Yoshimoto, M.; Tokimura, S.; Kurosawa, S. Characteristics of the series resonant frequency shift of a quartz crystal microbalance in electrolyte solutions. *Analyst* **2006**, *131*, 1175–1182.